Fusion probabilities in the reactions ^{40,48}Ca + ^{238}U at energies around the Coulomb barrier

K. Nishio,[1] S. Mitsuoka,[1] I. Nishinaka,[1] H. Makii,[1] Y. Wakabayashi,[2] H. Ikezoe,[1] K. Hirose,[3] T. Ohtsuki,[3] Y. Aritomo,[1,4] and S. Hofmann[5,6]

[1]*Advanced Science Research Center, Japan Atomic Energy Agency, Tokai, Ibaraki 319-1195, Japan*
[2]*Nishina Center for Accelerator-Based Science, RIKEN, Wako, Saitama 351-0198, Japan*
[3]*Resarch Center for Electron Photon Science, Tohoku University, 982-0826, Japan*
[4]*Flerov Laboratory of Nuclear Reactions, 141 980 Dubna, Russia*
[5]*GSI Helmholtzzentrum für Schwerionenforschung, 64291 Darmstadt, Germany*
[6]*Institut für Kernphysik, Goethe-Universität Frankfurt, 60438 Frankfurt am Main, Germany*

(Received 31 August 2011; revised manuscript received 24 July 2012; published 18 September 2012)

Fission cross sections and fission fragment mass distributions were measured in the reactions of ^{40}Ca + ^{238}U and ^{48}Ca + ^{238}U at energies around the Coulomb barrier. Fusion probabilities were calculated based on the fluctuation dissipation model. The measured mass distributions for both reactions showed an asymmetric shape at low incident energies, whereas the distribution changed to a flat shape at higher energies. The variation of the mass distribution is explained by a change of the ratio between fusion and quasifission with nuclear orientation. The calculation reproduced the mass distributions and their energy dependence. The trajectories for fusion-fission were used to determine the fusion probability. Fusion probabilities for both reactions are identical as function of the center-of-mass energy ($E_{\mathrm{c.m.}}$), but they differ when plotted as function of the excitation energy (E^*). Evaporation residue cross sections were calculated for the reaction ^{48}Ca + ^{238}U using a statistical model and the obtained fusion cross sections as input values. The results are compared to experimental data.

DOI: 10.1103/PhysRevC.86.034608 PACS number(s): 25.70.Jj, 25.85.Ge, 24.75.+i, 27.90.+b

I. INTRODUCTION

Production of superheavy nuclei (SHN) is one of the most challenging issues in nuclear physics to pin down the location of closed shell structures in the extreme region of the chart of nuclei as well as to investigate the atomic properties [1–3]. The understanding of the fusion process is important to estimate the cross sections to produce new SHN. In heavy-ion induced reactions, quasifission competes with fusion, so that the fusion cross section is lower than the capture cross section when the colliding nuclei penetrate or overcome the Coulomb barrier. Measurement of the evaporation residue (ER) cross sections gives information on the fusion probability. However, because of the low production rate for SHN, available data with high statistical accuracy are limited. The other possible way to obtain information on fusion is to measure the fission properties. Fission fragments have two origins which have different properties: Quasifission and compound-nucleus fission (fusion-fission). In reactions using actinide target nuclei, quasifission and fusion-fission generate fragments with different mass asymmetry. Quasifission shows an asymmetric mass distribution with fragments in the vicinity of the doubly closed shell nuclei ^{208}Pb and ^{78}Ni, whereas fusion-fission shows a symmetric distribution [4–9]. The measured fission spectra contain information on fusion and/or quasifission. A fusion probability (P_{fus}) can be determined with a help of theoretical model as presented in Ref. [10], where quasifission and fusion-fission are described in the same formula. Such an attempt was made in the study of ^{30}Si + ^{238}U [11] and ^{34}S + ^{238}U [12]. In these reactions, measured fragment mass distributions change significantly with respect to the incident beam energy due to the effects of nuclear orientation on the reaction arising from the prolate deformation of ^{238}U [7]. The mass distributions were reproduced by a calculation based on a fluctuation-dissipation model [13], where orientation effects were taken into account, and the fusion probabilities were determined by choosing trajectories for fusion-fission. The obtained fusion probabilities were consistent with the measured cross sections for seaborgium and hassium isotopes produced in the ^{30}Si + ^{238}U and ^{34}S + ^{238}U reactions, respectively.

In this article, we report on a similar study of the reactions of ^{40}Ca + ^{238}U and ^{48}Ca + ^{238}U and the resulting fusion probabilities. Experimentally, the ^{48}Ca + ^{238}U reaction was used for the synthesis of relatively neutron-rich isotopes of element 112 [14,15]. The study for ^{40}Ca + ^{238}U was intended to search for effects of the projectile's neutron number on fusion. The two reactions also exhibit differences of the fusion Q values: −138.6 MeV in the case of ^{40}Ca + ^{238}U and −159.1 MeV in the case of ^{48}Ca + ^{238}U, which results in a 20.5 MeV difference of the excitation energies of the compound nuclei at the same center-of-mass energy $E_{\mathrm{c.m.}}$.

II. EXPERIMENTAL DETAILS

The experiment was carried out using ^{40,48}Ca beams supplied from the JAEA tandem-booster accelerator. The experimental setup and the analysis method are similar to that described in Ref. [7]. Beam energies were varied in the region of the Coulomb barrier. Typical beam intensities were 0.5–1.0 particle-nA (1 particle-nA = 6.242×10^9 particles/s). The ^{238}U target was prepared by electrodeposition of natural UO_2 on a nickel foil of 90 μg/cm^2 thickness. The ^{238}U content was 80 μg/cm^2.

Both fission fragments were detected in coincidence using position-sensitive multiwire proportional counters (MWPCs). The MWPCs had an active area of 200 mm horizontally by 120 mm vertically. The detectors were located on both sides of the target at a distance of 223 mm and at angles of −60.0°

for MWPC1 and +60.0° for MWPC2 with respect to the beam direction. Each MWPC covered an emission angle of ±24.2° horizontally around the detector center. The detectors were operated with isobutane gas at a pressure of 3 Torr.

The time difference, ΔT, between the signals from two MWPCs was recorded. The signals from both MWPCs contain information on the energy deposition, ΔE_1 and ΔE_2, of particles traversing through the active region between the electrodes. From the position of the fragment, the emission angle for each fragment was determined. In the analysis, we separated fission events from reactions having the momentum of the projectile fully transferred to the composite system (full momentum transfer FMT) from fission fragments of nuclei around ^{238}U produced by nucleon transfer reactions. This was achieved by constructing the folding angle $\theta_{\rm fold} = \theta_1 + \theta_2$ and the sum of out-of-plane angles $\phi_{\rm sum} = \phi_1 + \phi_2$.

The fragment mass was determined by applying the conservation law for momentum and mass with the assumption that the mass of the composite system ($A_{\rm c}$) is equal to the sum of the projectile and target masses. The calibration was made by using the coincidence events from elastic collisions. The mass resolution at FWHM was 4.8. Two dimensional spectra of total kinetic energy (TKE) versus mass (A) were constructed. Fission events were separated in the A-TKE plane and used for obtaining the fission cross sections and fragment mass distributions.

III. EXPERIMENTAL RESULTS

The cross sections for FMT fission ($\sigma_{\rm fiss}$) of ^{40}Ca + ^{238}U and ^{48}Ca + ^{238}U as a function of $E_{\rm c.m.}$ are shown in Fig. 1. The cross sections were obtained by fitting the fragment angular distributions as function of the center-of-mass angle $d\sigma_{\rm fiss}/d\Omega(\theta_{\rm c.m.})$ of $70^\circ \leqslant \theta_{\rm c.m.} \leqslant 100^\circ$ to a function given in Ref. [16] and integrating it over the angle. The errors include systematic uncertainties arising from the limited angular range covered as well as statistical uncertainties. Most composite systems produced by the FMT process disintegrate as fission (fusion-fission and quasifission) in a reaction leading to a heavy system. The FMT fission cross sections in the studied reactions are thus nearly equal to the capture cross sections ($\sigma_{\rm cap}$).

In order to visualize the effects of the static deformation of ^{238}U on the fission (capture) cross section, we show in Fig. 1 calculated data using the code CCDEGEN [17]. The dashed curve is the result without considering deformation of ^{238}U (one-dimensional barrier penetration model). For ^{40}Ca + ^{238}U, this calculation reproduces the measured data above the Coulomb barrier $V_{\rm B} = 198.6$ MeV except the highest energy point at $E_{\rm c.m.} = 230.0$ MeV. The data in the sub-barrier region at $E_{\rm c.m.} \leqslant V_{\rm B}$ can be explained by taking into account the deformation of ^{238}U $(\beta_2, \beta_4) = (0.275, 0.050)$ (solid curve) [18]. For ^{48}Ca + ^{238}U, the calculation reproduces two data points at $E_{\rm c.m.} = 200.0$ and 210.0 MeV above $V_{\rm B} = 194.5$ MeV. The calculation overestimates the cross section in the higher energy region at $E_{\rm c.m.} > 210.0$ MeV. The sub-barrier data of ^{48}Ca + ^{238}U is closer to the calculation taking into account the deformation of ^{238}U, however, the calculation overestimates the measured data.

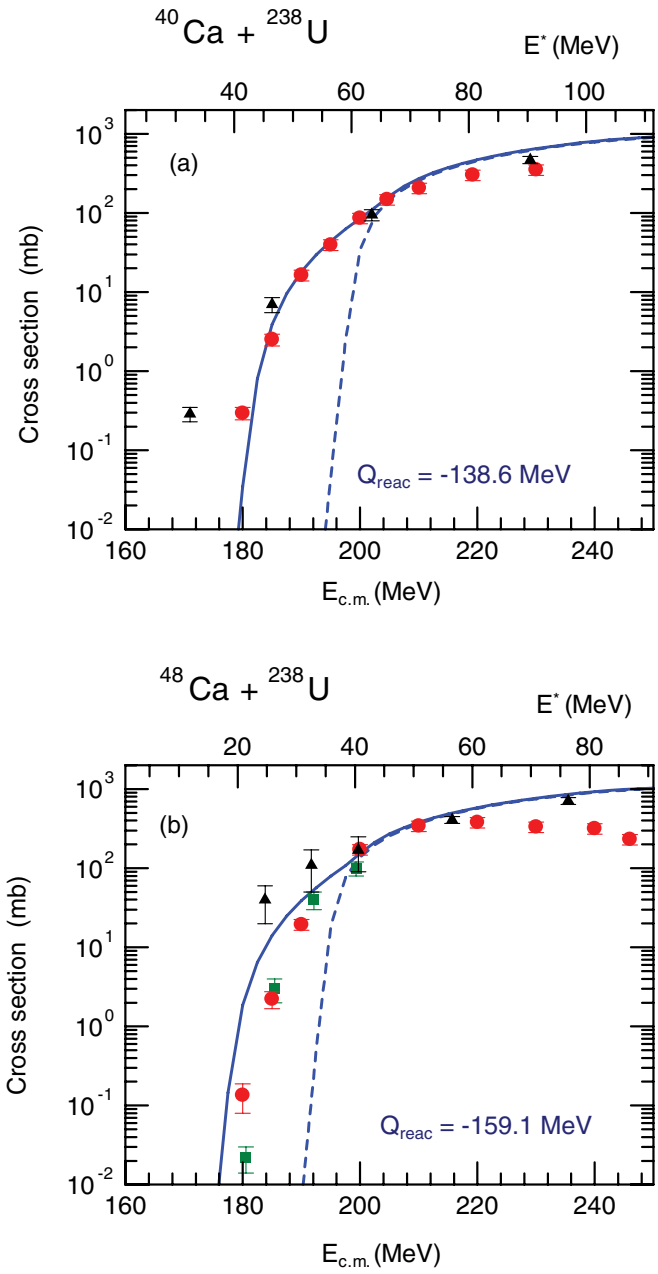

FIG. 1. (Color online) Cross sections for full momentum transfer (FMT) fissions of the reactions (a) ^{40}Ca + ^{238}U and (b) ^{48}Ca + ^{238}U plotted as a function of the center-of-mass energy (solid circles). Solid and dashed curves are the model calculations with and without taking into account the prolate deformation of ^{238}U. Data given in Refs. [6] (squares) and [4] (triangles) are also shown.

Capture cross sections at energies around the Coulomb barrier were also measured in inverse-kinematic experiment using ^{238}U beams and calcium targets [4,5]. The data are shown together with our data in Fig. 1. At low energy, these values are significantly larger than the present data. A possible reason is a contamination by transfer-induced fission, which can be significantly larger than FMT fission in the sub-barrier region. The results given in Ref. [6] using normal kinematics with a ^{48}Ca beam are in good agreement with the present results.

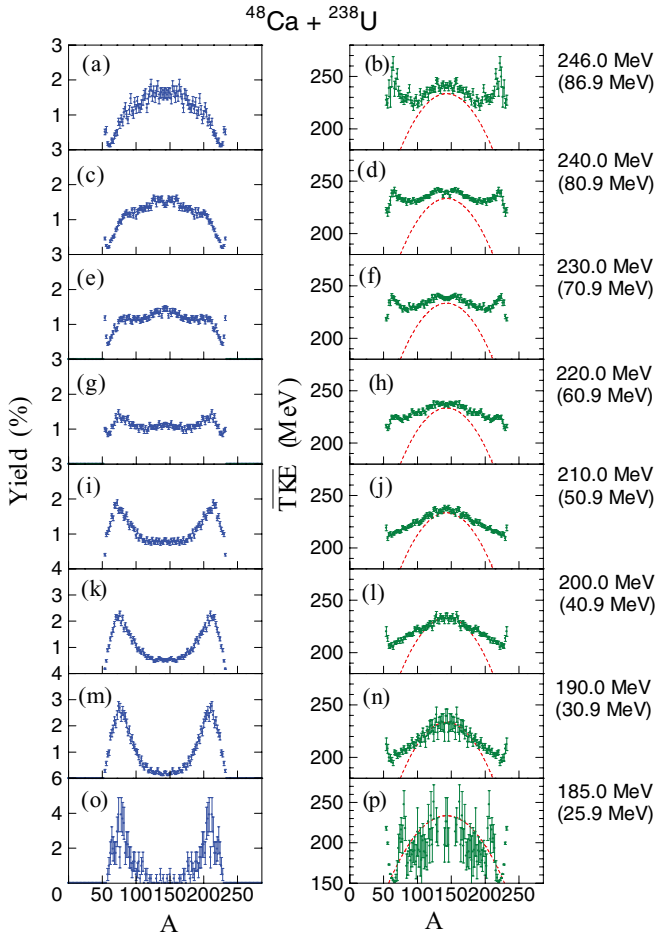

FIG. 2. (Color online) Fission fragment mass distribution (left) and average total kinetic energy $\overline{TKE}$ (right) in the reaction of $^{48}Ca + ^{238}U$. Beam energy $E_{c.m.}$ (excitation energy E^* in parenthesis) are indicated. Dashed curves represent calculated TKE values based on the Viola formula [19].

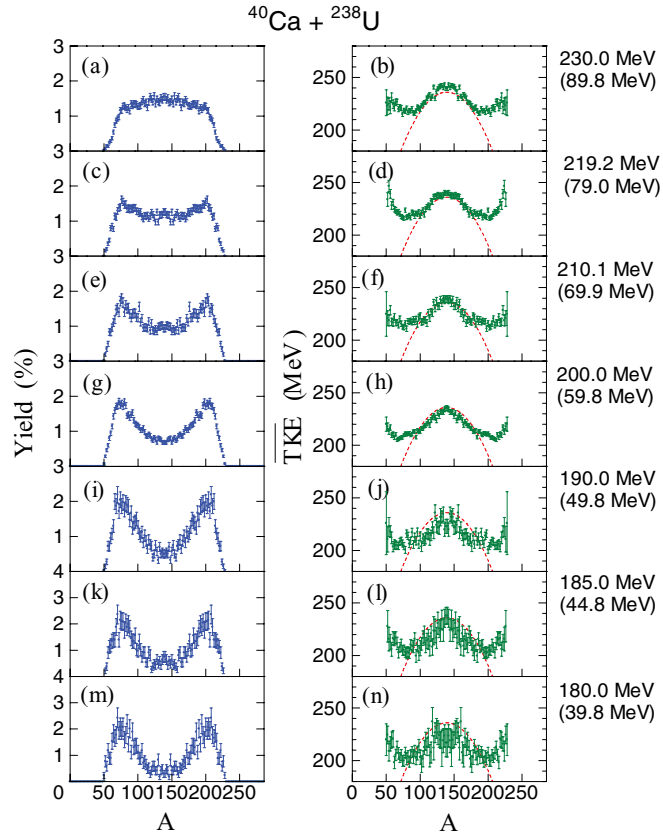

FIG. 3. (Color online) Same as Fig. 2 but in the reaction of $^{40}Ca + ^{238}U$.

Figures 2 and 3 show fragment mass yields for FMT fission of the reactions $^{48}Ca + ^{238}U$ and $^{40}Ca + ^{238}U$, respectively. The spectra are normalized such that the total area of each spectrum summed over the mass range is 200%. The data cover the detection angle of fission fragments from $\theta_{c.m.} = 65^\circ$ to 115°. It is known that in irradiations of actinide target nuclei with heavier projectiles a forward-backward mass asymmetry is measured as result of fragments from quasifission. An example is found in the study of $^{32}S + ^{232}Th$ [8], where fragment mass and emission angle were measured within $\theta_{c.m.} = 45^\circ$ to 135°. From the present experiment we cannot extract such information due to smaller coverage of the detection angle. However, our attempt is to determine the fusion probability based on the FMT fission in a wide energy range from the above-barrier to the sub-barrier region. The separation between FMT fission and nucleon-transfer induced fission is important especially at low energies as follows. In the present measurement, yields for FMT fission events among all fission events are 0.92 at $E_{c.m.} = 220.0$ MeV and 0.30 at 185.0 MeV in the $^{48}Ca + ^{238}U$ reaction. The $^{40}Ca + ^{238}U$ reaction exhibits significantly smaller values of 0.73 at $E_{c.m.} = 219.2$ MeV and 0.075 at 185.0 MeV. A good separation of FMT fission from transfer-induced fissions can be achieved around $\theta_{c.m.} = 90^\circ$ using the difference of folding angles. The separation is more difficult in the case of fission fragments emitted near 0° and 180° in the laboratory system. However, the limited angular range covered in our experiment does not change the conclusions.

In the $^{48}Ca + ^{238}U$ reaction, the FMT fission yields have a broad mass distribution at $E_{c.m.} = 246.0$, 240.0, and 230.0 MeV with a small hump in the mass-symmetry region. Towards lower incident energies, the asymmetric fission modes around $A_L \approx 74$ and $A_H \approx 212$ grow, and the distributions are increasingly dominated by asymmetric fission. A similar trend is also observed in the $^{40}Ca + ^{238}U$ reaction, but the asymmetric fission is centered at $A_L \approx 74$ and $A_H \approx 204$. We realize that in the case of quasifission the different projectile masses, 40 u and 48 u, affects the localization of the distribution of the heavy fragment and not that of the lighter one.

As discussed in Ref. [7], the observed variation of the mass distribution with incident energy is due to orientation effects on the competition between fusion and quasifission. At sub-barrier energy, projectiles reach contact with the prolate-deformed ^{238}U nucleus only in polar collisions, and the reaction start from a pronounced elongated deformation. This results in a larger quasifission probability than in the case of reactions starting from an equatorial configuration which

is obtained at higher beam energies. This interpretation also holds for the reactions ^{40,48}Ca + ^{238}U studied here.

The average total kinetic energy ($\overline{TKE}$) for each mass bin is also plotted in Figs. 2 and 3. The data are compared with the curve $\overline{TKE}(A) = TKE_0(A_c - A)A/(A_c/2)^2$, where the TKE_0 is obtained from the Viola formula (Eq. (3) in Ref. [19]). For the ^{48}Ca + ^{238}U reaction, the measured $\overline{TKE}$ data agree with the Viola-curve in the symmetric mass region of A = 112–174 at energies $E_{c.m.} = 190.0 \sim 220.0$ MeV, whereas at $E_{c.m.} = 230.0 \sim 246.0$ MeV the experimental data are slightly larger than the Viola curve. For the ^{40}Ca + ^{238}U reaction, the $\overline{TKE}$ data agree in the region A = 104–174 except for the lowest energy data at $E_{c.m.} = 180.0 \sim 190.0$ MeV, where the measured $\overline{TKE}$ data is below the Viola curve.

Towards larger mass asymmetries outside the above-mentioned mass ranges, the measured $\overline{TKE}$ have larger values than that of the Viola curve. At a mass asymmetry corresponding to the peak of the asymmetric fission mode, the measured $\overline{TKE}(A = 212)$ in the ^{48}Ca + ^{238}U reaction at $E_{c.m.} = 210.0$ MeV is 36 MeV larger than the calculated one. The difference is 28 MeV for ^{40}Ca + ^{238}U at $A = 204$ and $E_{c.m.} = 210.1$ MeV. Applying the simple idea that the total kinetic energy is equal to the Coulomb energy at the scission point represented by $V_C \propto Z_1Z_2/R$, then the distance R between the charge centers of the nascent fragments is 15–20% shorter in the case of mass asymmetric fission than in the case of symmetric fission. To obtain a higher $\overline{TKE}$ value, the fragments at scission must be less deformed. This suggests a particular trajectory on the potential energy landscape before reaching the scission point.

Comparing the measured mass distributions of the reactions ^{48}Ca + ^{238}U and ^{40}Ca + ^{238}U as shown in Figs. 2 and 3, one observes a good agreement between the shapes of the mass distributions, when incident energies ($E_{c.m.}$) are the same. This is not the case for the distributions at the same excitation energy (E^*). This means that the yields of the two different scission configurations, the mass-symmetric fission with elongated fragment shape and the asymmetric quasifission with less-deformed shape, are determined by the beam energy $E_{c.m.}$. This can be explained by the height of the conditional saddle point V_{con} as well as the incident beam energy. The conditional saddle is the saddle of composite system at a frozen (entrance channel) mass asymmetry [20]. The dinuclear system has to surmount the conditional saddle point in order to from the compound nucleus. A system rebounded by V_{con} disintegrates as quasifission with mass asymmetry. The excitation energy E^* relative to V_{con} should influence the probability for mass-symmetric fission and quasifission. In a two-center shell model [21], the V_{con} values measured from the ground state of the compound nuclei ^{278}Cn (^{40}Ca + ^{238}U) and ^{286}Cn (^{48}Ca + ^{238}U) are 56 MeV and 30 MeV, respectively. The former reaction needs an excitation energy 26 MeV higher than the latter reaction for having the same probability to overcome the V_{con}. However, due to the 20.5 MeV higher Q value of the ^{40}Ca + ^{238}U reaction than ^{40}Ca + ^{238}U, the ^{40}Ca + ^{238}U reaction needs only a 5.5 MeV higher value of $E_{c.m.}$ than ^{48}Ca + ^{238}U in order to yield a similar probability for symmetric-fission and/or mass-asymmetric quasifission.

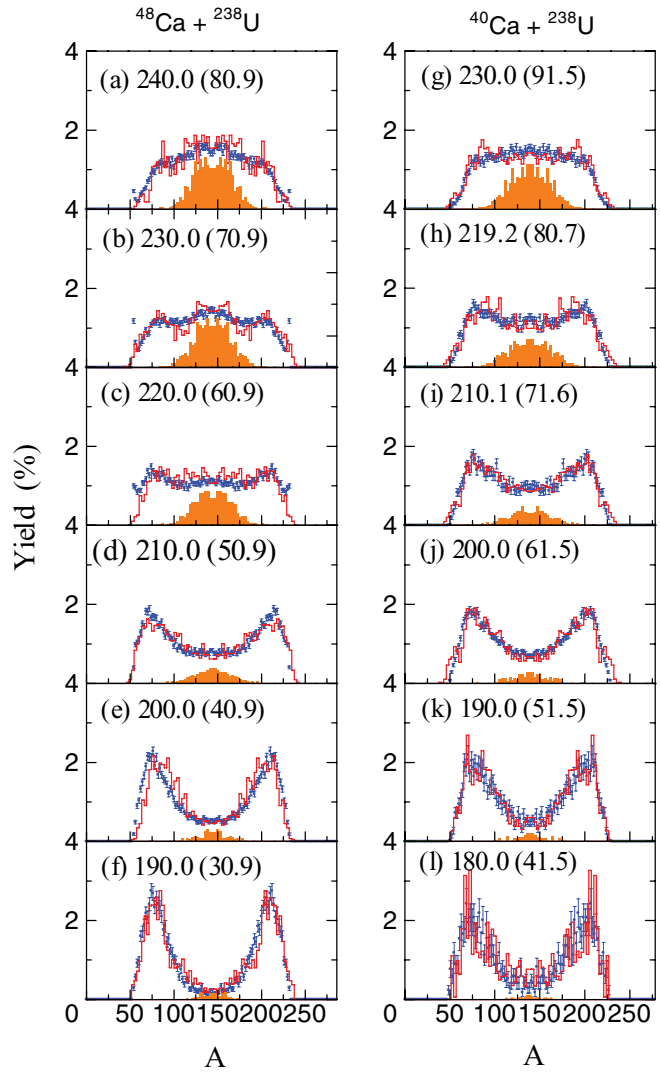

FIG. 4. (Color online) Calculated fission fragment mass distributions are compared with the experimental data. Beam energy $E_{c.m.}$ (excitation energy E^* in parentheses) are indicated. The filled spectrum shows the calculated fusion-fission events.

IV. DISCUSSIONS

A calculation based on the fluctuation-dissipation model was carried out to determine the fusion probability P_{fus} [13]. A Langevin equation was solved to track the shape evolution with time. The calculation started from the impact of the projectile on the target nucleus and ended at scission. The results are shown in Fig. 4, where the histogram represents all fission fragments. The calculation reproduces the measured spectra in the entire energy range for the ^{40,48}Ca + ^{238}U reactions.

Fusion-fission events are assigned by choosing trajectories for fission after formation of the compound nucleus. The corresponding spectra are shown in Fig. 4 by the filled area. Fission from the compound nucleus has a mass-symmetric distribution with the Gaussian shape. It is found in the analysis that the standard deviation σ_m decreases toward the low incident energy that the σ_m is 22u at $E_{c.m.} = 240.0$ MeV and 15 u at 190.0 MeV for ^{48}Ca + ^{238}U. For the reaction ^{40}Ca + ^{238}U, the

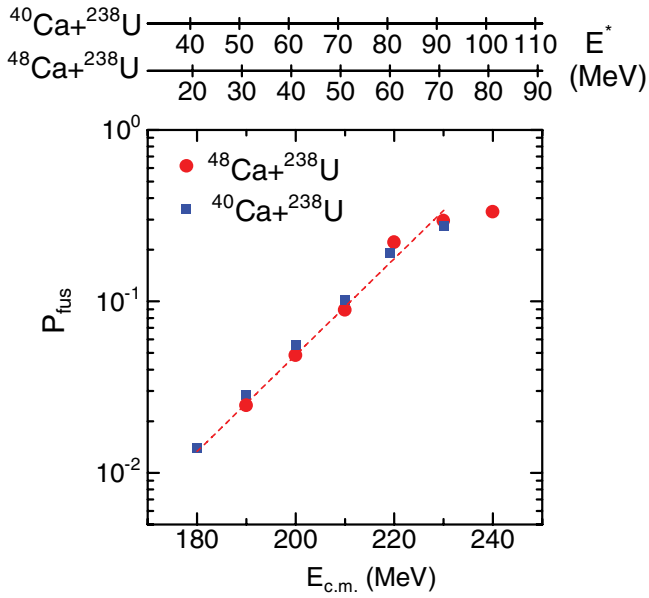

FIG. 5. (Color online) Fusion probabilities for ^{40}Ca + ^{238}U (rectangle) and ^{48}Ca + ^{238}U (circle) plotted as a function of center-of-mass energy. Excitation energies of compound nucleus are also shown.

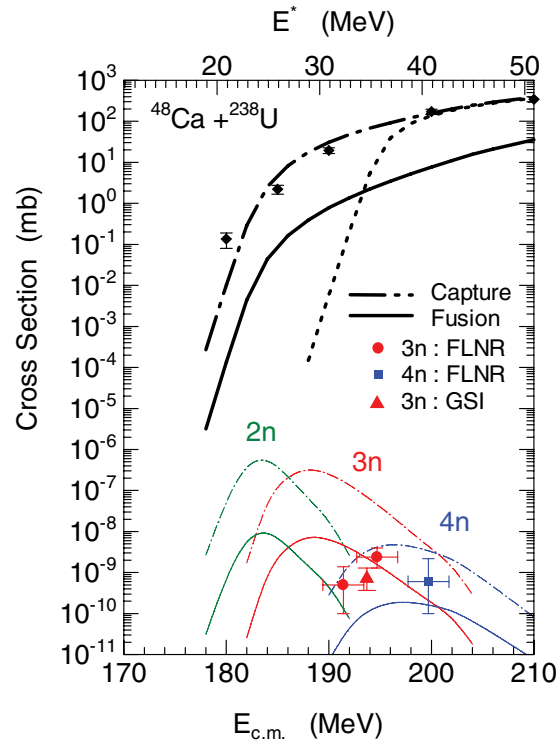

FIG. 6. (Color online) Measured fission cross sections (solid diamond) in the ^{48}Ca + ^{238}U reaction are compared to the calculated capture cross sections. The bold dash-dotted curve and the bold dotted curves are results with and without considering deformation of ^{238}U. Fusion cross sections are shown by the bold solid curve. The thin solid curves are the ER cross sections calculated by inputting the fusion cross sections to the statistical model code. The results without hindrance of fusion are shown by the thin dot-dashed curves. Experimental ER cross section of 3n evaporation channel are taken at FLNR [1,14] (solid circle) and GSI [15] (solid triangle). The data for the 4n channel taken at FLNR [1,14] is shown by a solid rectangle.

σ_m is 23 u at $E_{c.m.} = 230.0$ MeV and 17 u at 180.0 MeV. This trend arises from the temperature dependent random force in the Langevin equation, which give rise to the smaller fluctuation in mass asymmetry of fission at low temperature.

Figure 5 shows the fusion probabilities P_{fus} determined from the ratio of calculated fusion-fission events to the calculated total fission events. The P_{fus} values increase exponentially with $E_{c.m.}$, and at a certain value of $E_{c.m.}$ the data for the two reactions, ^{40}Ca + ^{238}U and ^{48}Ca + ^{238}U, are almost the same. However due to the large difference of the fusion Q values P_{fus} is 3.8 times larger in the case of ^{48}Ca + ^{238}U than in the case of ^{40}Ca + ^{238}U at a certain value of E^*.

It is obvious from the comparison shown in Fig. 4 that not all of the symmetric fission fragments originate from the compound nucleus. It is argued in the discussion in Refs. [8,12] that reactions leading to mass-symmetric fission fragments are not necessarily due to compound-nucleus formation when actinide targets are irradiated with sulfur beams. In the reaction ^{34}S + ^{238}U, the yield of fusion-fission fragments was obtained to be 0.14 $\sim$ 0.20 from the total amount of mass-symmetric fission events [12]. Calculations using the Langevin equation showed that deep-quasifission (DQF) also produces symmetric quasifission fragments [21]. In DQF, mass-asymmetry and charge-center distance of the reaction partner approach values close to the compound nucleus, but the system develops into the direction of fission without reaching the properties of an equilibrated compound nucleus. On the other hand, quasifission takes place immediately after nuclear contact within a relatively short time, and thus the fragments have a mass asymmetry close to that of the entrance channel.

In the ^{40}Ca + ^{238}U reaction, the yield for fusion-fission events among mass-symmetric fission with $A_c/2 - 40 < A < A_c/2 + 40$ increases exponentially from 0.09 at $E_{c.m.} =$ 190.0 MeV to 0.50 at $E_{c.m.} = 230.0$ MeV, which means that the QDF component decreases with incident energy. The corresponding yield in the ^{48}Ca + ^{238}U reaction also exhibits an increasing trend from 0.11 at $E_{c.m.} = 190.0$ MeV to 0.56 at $E_{c.m.} = 230.0$ MeV. The calculation also shows that the DQF yielding mass symmetric fission has nearly the same values for both reactions at the same incident energy, $E_{c.m.}$.

The reaction ^{48}Ca + ^{238}U was used for production of the isotopes ^{283}Cn(3n) and ^{282}Cn(4n) [1,14,15]. Using the capture cross sections and the fusion probabilities obtained in our experiment, we calculated the ER cross sections. The survival probability of the excited compound nucleus was calculated with the code HIVAP [22]. The partial cross sections $\sigma(L; E_{c.m.})$ were determined by the code given in Ref. [17], where the deformation of ^{238}U was modified from $(\beta_2, \beta_4) = (0.275, 0.050)$ to $(0.270, 0.00)$ such that the calculated σ_{cap} reasonable reproduce the measured fission cross sections. Figure 6 summarizes the results. The bold dash-dotted curve is the calculated σ_{cap}. These data were multiplied by P_{fus} given in Fig. 5 to yield the fusion cross sections (bold solid curve). The P_{fus} values were obtained by fitting an exponential function to the data points (dashed curve in Fig. 5). As the isotopes ^{282,283}Cn were produced in the energy interval of

$E_{\mathrm{c.m.}} = 190$–200 MeV, the corresponding P_{fus} values are 0.025–0.048.

The thin solid curves in Fig. 6 show the ER cross sections for $2n$, $3n$, and $4n$ channels calculated with the fusion cross sections as discussed before (bold solid curve in Fig. 6). The ER cross sections calculated without hindrance of fusion (bold dash-dotted curve in Fig. 6) are given by the thin dash-dotted curves. In the statistical model calculation, the binding energies of neutron, proton, and α particles were taken from the mass table [23].

The ER cross sections depend strongly on the fission barrier height B_{f}. The model dependent variations of B_{f} values are as large as $\Delta B_{\mathrm{f}} = 3 \sim 4$ MeV [1]. In the present calculation, the B_{f} values are assumed to be equal to the negative of the shell correction energy at the ground state. These values are taken from Ref. [23], but multiplied with 0.7 in order to reproduce the maximum cross section for ^{283}Cn($3n$) measured at $E^* = 35.0$ MeV [1,14]. The $3n$ cross section of 0.72 pb measured at the GSI-SHIP [15] at $E_{\mathrm{c.m.}} = 193.7$ MeV is slightly below the FLNR value.

The cross section of 0.6 pb obtained for the $4n$ channel at the higher incident energy ($E^* = 39.8$ MeV) at FLNR also agrees with the calculation within the statistical uncertainty. However, the cross section for the $3n$ channel taken at the lower energy of $E^* = 31.4$ MeV at FLNR is smaller than the calculated value.

The experimental data points for ERs seem to show a maximum cross section in between $E^* = 32$ and 36 MeV for $3n$ evaporation. The present analysis, however, predicts the maximum cross section for $3n$ evaporation at $E^* = 30$ MeV. The energy region which could be used for heavy-element synthesis is predicted to extend down to $E^* = 25$ MeV, where the $2n$ channel has its maximum.

It should be noted that the absolute values of the calculated ER cross sections depend strongly on the fission barrier height and other parameters in the code. However, the relative values of the excitation function should not change so drastically when fission barriers and binding energies of one and the same mass model are used. The excitation function of P_{fus} itself could also have uncertainties of the absolute values, which are associated with the definition of the shape of the compound nucleus (fusion box). Nevertheless, in so far as we are using the same fusion box for all incident energies in the calculation, the dependence of P_{fus} on $E_{\mathrm{c.m.}}$ does not change essentially. Our calculation, which results in reasonable ER cross sections in the $E^* = 35$–40 MeV region, reveals that measurement could be extended down to $E^* = 25$ MeV. This prediction is based on the experimental results that the mass distributions change smoothly from the above barrier to the sub-barrier energy region. It would be interesting to complete the excitation function for synthesis of copernicium isotopes at lower incident energies than used so far.

V. CONCLUSIONS

Fission fragment mass and TKE distributions were measured in the reactions ^{40}Ca + ^{238}U and ^{48}Ca + ^{238}U. Fusion probabilities were obtained from the measured fission mass distribution with a help of fluctuation-dissipation model using Langevin equations. Fusion probabilities for both reactions give identical values when they are compared at the same incident energy. Using the fusion probabilities obtained in the ^{48}Ca + ^{238}U reaction, we estimated the trend of the cross section for the copernicium isotopes produced by $2n$, $3n$, and $4n$ evaporation channels. The calculation does not show a sharp drop of the cross section below $E^* = 33$ MeV but reveals values large enough for production of superheavy nuclei using current techniques at excitation energies down to $E^* = 25$ MeV, at which the $2n$ channel has a cross section maximum. It would be an important task to search for copernicium isotopes at low incident energies in order to better understand the fusion process.

ACKNOWLEDGMENTS

The authors thank the crew of the JAEA-tandem facility for the beam operation. Special thanks are due to Dr. T. Ishii for the preparation of calcium material for extraction of the beams from the negative ion source. The numerical calculations were carried out on SR16000 at YITP at Kyoto University. This work was supported by a Grant-in-Aid for Scientific Research of the Japan Society for the Promotion of Science.

[1] Yu. Ts. Oganessian, J. Phys. G **34**, R165 (2007).
[2] S. Hofmann and G. Münzenberg, Rev. Mod. Phys. **72**, 733 (2000).
[3] K. Morita *et al.*, J. Phys. Soc. Jpn. **73**, 2593 (2004).
[4] W. Q. Shen *et al.*, Phys. Rev. C **36**, 115 (1987).
[5] J. Tõke *et al.*, Nucl. Phys. A **440**, 327 (1985).
[6] M. G. Itkis *et al.*, Nucl. Phys. A **787**, 150c (2007).
[7] K. Nishio *et al.*, Phys. Rev. C **77**, 064607 (2008).
[8] D. J. Hinde, R. du Rietz, M. Dasgupta, R. G. Thomas, and L. R. Gasques, Phys. Rev. Lett. **101**, 092701 (2008).
[9] I. M. Itkis *et al.*, Phys. Rev. C **83**, 064613 (2011).
[10] V. Zagrebaev and W. Greiner, J. Phys. G **31**, 825 (2005).
[11] K. Nishio *et al.*, Phys. Rev. C **82**, 044604 (2010).
[12] K. Nishio *et al.*, Phys. Rev. C **82**, 024611 (2010).
[13] Y. Aritomo, K. Hagino, K. Nishio, and S. Chiba, Phys. Rev. C **85**, 044614 (2012).
[14] Yu. Ts. Oganessian *et al.*, Phys. Rev. C **70**, 064609 (2004).
[15] S. Hofmann *et al.*, Eur. Phys. J. A **32**, 251 (2007).
[16] R. Vandenbosch and J. R. Huizenga, *Nuclear Fisson* (Academic Press, New York, 1973).
[17] Modified version of the CCFULL code, K. Hagino *et al.*, Computer Phys. Comm. **123**, 143 (1999).
[18] K. Nishio *et al.*, Phys. Rev. Lett. **93**, 162701 (2004).
[19] V. E. Viola, K. Kwiatkowski, and M. Walker, Phys. Rev. C **31**, 1550 (1985).
[20] W. J. Swiatecki, Nucl. Phys. A **376**, 275 (1982).
[21] Y. Aritomo and M. Ohta, Nucl. Phys. A **753**, 152 (2005).
[22] W. Reisdorf and M. Schädel, Z. Phys. A **343**, 47 (1992).
[23] P. Möller *et al.*, At. Data Nucl. Data Tables **59**, 185 (1995).